Synthesis and Characterization of Ruthenium Complexes with Two Fluorinated Amino Alkoxide Chelates. The Quest To Design Suitable MOCVD Source Reagents

Ying-Hui Lai,[†] Tsung-Yi Chou,[†] Yi-Hwa Song,[†] Chao-Shiuan Liu,[†] Yun Chi,*[,†] Arthur J. Carty,*[,‡] Shie-Ming Peng,[§] and Gene-Hsiang Lee[§]

Department of Chemistry, National Tsing Hua University, Hsinchu 30013, Taiwan, Steacie Institute for Molecular Sciences, National Research Council Canada, 100 Sussex Drive, Ottawa, Ontario K1A 0R6, Canada, and Department of Chemistry and Instrumentation Center, National Taiwan University, Taipei 10764, Taiwan

Received January 22, 2003. Revised Manuscript Received March 31, 2003

The synthesis and characterization of ruthenium complexes $[Ru(CO)_2(amak)_2]$ and $[Ru(COD)(amak)_2]$ (where COD = 1,4-cyclooctadiene) are reported, where (amak)H is an abbreviation for a series of fluorinated amino alcohol ligands with formula $HOC(CF_3)_2CH_2NHR$, where R = H, Me, Et, and $(CH_2)_2OMe$. The carbonyl complex $[Ru(CO)_2(amak1)_2]$ (**1** with R = H) was examined by X-ray diffraction (XRD), showing an octahedral coordination for the Ru atom, with two cis carbonyl ligands and two amino alkoxide chelates. For the COD complexes $[Ru(COD)(amak1)_2]$ (**3** with R = H) and $[Ru(COD)(amak3)_2]$ (**4** with R = Et), the structural analysis indicated the existence of two distinct spatial arrangements of amino alkoxide chelates with respect to the coordinated COD ligand, depending on the type of amino group selected. All of these complexes show good volatility and thermal stability. For complexes **2** and **4**, which are more volatile and low-melting, chemical vapor deposition (CVD) experiments were conducted at temperatures of 325−425 °C, using both H_2 and a mixture of 2% O_2 in argon as the carrier gas. Scanning electron micrographs (SEMs) were taken to reveal the surface morphologies; these Ru thin films were found to contain low levels of carbon and oxygen impurities, as measured by X-ray photoelectron spectroscopy (XPS).

Introduction

Thin film materials based on Ru metal and RuO_2 are used extensively for fabricating electrodes or noncorrosive diffusion barriers for next-generation tantalum oxide (Ta_2O_5), barium strontium titanate, and lead zirconate titanate based nonvolatile random access memory devices.[1] Among various deposition methods that have come under scrutiny, CVD has become increasingly attractive[2] because it allows direct deposition of the Ru-containing material on the substrate and greatly simplifies the deposition process. However, the study of Ru CVD processes has been somewhat limited by the lack of suitable precursors because most of the available Ru complexes either are poorly volatile, as exemplified by the binary carbonyl complex $Ru_3(CO)_{12}$,[3] ruthenocene,[4] and tris-β-diketonate coordination complexes such as $Ru(acac)_3$, $Ru(tfac)_3$, and $Ru(tmhd)_3$, tfac = 1,1,1-trifluoro-2,4-pentanedionate, and tmhd = 2,2,6,6-tetramethyl-3,5-heptanedionate,[5] or suffer from poor stability during storage under ambient conditions, making their preparation and handling a very tedious task. The second class of source compounds includes the unstable carbonyl complex $Ru(CO)_5$,[6] the metal oxide RuO_4,[7] the bis-allyl complex $Ru(C_3H_5)_2(COD)$, where COD = 1,4-cyclooctadiene,[8] and the alkene complex (η^6-C_6H_6)Ru-

* To whom correspondence should be addressed. Fax: (886) 3 572-0864. E-mail: ychi@mx.nthu.edu.tw.
[†] National Tsing Hua University.
[‡] National Research Council Canada.
[§] National Taiwan University.

(1) Yamamichi, S.; Lesaicherre, P.-Y.; Yamaguchi, H.; Takemura, K.; Sone, S.; Yabuta, H.; Sato, K.; Tamura, T.; Nakajima, K.; Ohnishi, S.; Tokashiki, K.; Hayashi, Y.; Kato, Y.; Miyasaka, Y.; Yoshida, M.; Ono, H. *IEEE Trans. Electron Devices* **1997**, *44*, 1076.
(2) (a) Gladfelter, W. L. *Chem. Mater.* **1993**, *5*, 1372. (b) Puddephatt, R. J. *Polyhedron* **1994**, *13*, 1233. (c) Vahlas, C.; Juarez, F.; Feurer, R.; Serp, P.; Caussat, B. *Chem. Vap. Deposition* **2002**, *8*, 127.
(3) (a) Smart, C. J.; Gulhati, A.; Reynolds, S. K. *Mater. Res. Soc. Symp. Proc.* **1995**, *363*, 207. (b) Boyd, E. P.; Ketchum, D. R.; Deng, H.; Shore, S. G. *Chem. Mater.* **1997**, *9*, 1154. (c) Choi, Y. C.; Lee, B. S. *Jpn. J. Appl. Phys.* **1999**, *38*, 4876.
(4) (a) Si, J.; Desu, S. B. *J. Mater. Res.* **1993**, *8*, 2644. (b) Shin, W.-C.; Yoon, S.-G. *J. Electrochem. Soc.* **1997**, *144*, 1055. (c) Aoyama, T.; Kiyotoshi, M.; Yamazaki, S.; Eguchi, K. *Jpn. J. Appl. Phys.* **1999**, *38*, 2194. (d) Park, S.-E.; Kim, H.-M.; Kim, K.-B.; Min, S.-H. *J. Electrochem. Soc.* **2000**, *147*, 203.
(5) (a) Hones, P.; Levy, F.; Gerfin, T.; Gratzel, M. *Chem. Vap. Deposition* **2000**, *6*, 193. (b) Bai, G.-R.; Wang, A.; Foster, C. M.; Vetrone, J. *Thin Solid Films* **1997**, *310*, 75. (c) Lee, J. M.; Shin, J. C.; Hwang, C. S.; Kim, H. J.; Suk, C.-G. *J. Vac. Sci. Technol.* **1998**, *16*, 2768. (d) Lee, D.-J.; Kang, S.-W.; Rhee, S.-W. *Thin Solid Films* **2002**, *413*, 237.
(6) Berry, A. D.; Brown, D. J.; Kaplan, R.; Cukauskas, E. J. *J. Vac. Sci. Technol. A* **1986**, *4*, 215.
(7) (a) Yuan, Z.; Puddephatt, R. J.; Sayer, M. *Chem. Mater.* **1993**, *5*, 908. (b) Sankar, J.; Sham, T. K.; Puddephatt, R. J. *J. Mater. Chem.* **1999**, *9*, 2439.
(8) (a) Barreca, D.; Buchberger, A.; Daolio, S.; Depero, L. E.; Fabrizio, M.; Morandini, F.; Rizzi, G. A.; Sangaletti, L.; Tondello, E. *Langmuir* **1999**, *15*, 4537. (b) Barison, S.; Barreca, D.; Daolio, S.; Fabrizio, M.; Tondello, E. *J. Mater. Chem.* **2002**, *12*, 1511.

10.1021/cm030029c CCC: $25.00
Published on Web 05/23/2003

(η^4-C_6H_8), where C_6H_8 = 1,3-cyclohexadiene.[9] However, these undesirable properties were partially resolved by Gladfelter and co-workers, who have used the carbonyl complex Ru(CO)4(hfb),[10] where hfb = hexafluoro-2-butyne, in depositing-reflective, high-purity Ru metal thin films at temperatures as low as 200 °C. Moreover, inclusion of a liquid source supply system using the ruthenocene derivative $Ru(C_5H_4Et)_2$ has also significantly improved the future prospects for the CVD approach,[11] by elimination of the problems of precursor long-term stability, while providing a constant rate of evaporation.

Recently, our group has initiated a program involving evaluation of new CVD source reagents, which prompted us to synthesize a series of complexes such as $[Ru(CO)_2(tmhd)_2]$ and $[Ru(CO)_2(hfac)_2]$, where hfac = hexafluoroacetylacetonate.[12] In contrast to Gladfelter's results, our compounds showed no tendency to dimerize upon heating in an inert atmosphere, which can greatly simplify the deposition mechanisms, making the precursors very suitable for depositing both Ru and RuO_2 thin films.[13] To extend this research endeavor, we have now designed and synthesized a new kind of carbonyl source reagent (**1** and **2**) as well as the COD derivatives (**3**−**5**), for which the central Ru metal cation is directly linked to two amino alkoxide chelates, while the other coordination sites are occupied by either a pair of cis CO ligands or a COD ligand (Chart 1). Studies on the basic chemical and structural properties of these complexes will be presented in this paper, with a special focus on those affecting CVD processing parameters. The potential application in materials research is also described in terms of the ease of preparation of various Ru thin films.

Chart 1

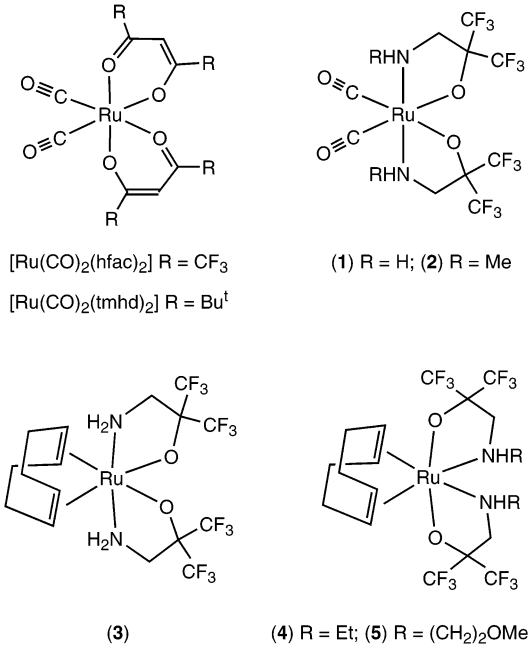

Experimental Section

General Information and Materials. Mass spectra were obtained on a JEOL SX-102A instrument operating in electron impact (EI) mode or fast atom bombardment mode. ^{1}H and ^{13}C NMR spectra were recorded on a Varian Mercury-400 or INOVA-500 instrument; chemical shifts are quoted with respect to the internal standard tetramethylsilane for ^{1}H and ^{13}C NMR data. Elemental analyses were carried out at the NSC Regional Instrumentation Center at National Cheng Kung University, Tainan, Taiwan. The ruthenium complex $[Ru(COD)Cl_2]_x$ was prepared according to the literature method,[14] and the amino alcohol ligands were prepared using a modified method developed in this laboratory.[15] All reactions were performed under nitrogen using anhydrous solvents or solvents treated with an appropriate drying reagent.

Identification of the as-deposited Ru thin films was carried out using an X-ray diffractometer with Cu Kα radiation. SEMs were recorded on a Hitachi S-4000 system. The electrical resistivity on films was measured by a four-point probe method at room temperature, for which the instrument is assembled using Keithley 2182 nanovoltmeter and a Keithley 2400 constant current source. The elemental composition was determined by XPS utilizing a Physical Electronics PHI 1600 system with an Al/Mg dual-anode X-ray source, and the XPS spectra were collected after 1−2 min of sputtering with argon at 4 keV until a constant composition was obtained. The relative content of carbon vs ruthenium metal was measured using least-squares deconvolution of the carbon 1s peak and the corresponding ruthenium $3d_{5/2}$ and $3d_{3/2}$ peaks, while those of the spectral deconvolution procedures were carried out using a nonlinear least-squares fitting program adopting mixed Gaussian−Lorentzian line shape and Shirley baselines.

Synthesis of Complex 1. A 160 mL stainless steel autoclave was charged with 1.53 g of amino alcohol (amak1)H, $HOC(CF_3)_2CH_2NH_2$ (7.77 mmol), 0.8 g of $Ru_3(CO)_{12}$ (1.25 mmol), and 50 mL of hexane. The autoclave was sealed, and the mixture was heated to 180 °C for 18 h. The red-orange solution was then evaporated under vacuum, and the crude product was purified by sublimation at 80 °C under a pressure of 150 mTorr, giving a light yellow solid. Recrystallization from a mixture of CH_2Cl_2 and methanol at room temperature afforded 0.67 g of colorless, needle-shaped compound $[Ru(CO)_2(amak1)_2]$ (**1**; 1.22 mmol, 33%).

Spectral data of **1**: MS (EI, ^{102}Ru) *m*/*z* 549 (M^+); IR (CH_2Cl_2) ν(CO) 2050 (s), 1972 (vs) cm^{-1}; ^{1}H NMR (500 MHz, methanol-d_4, 298 K) δ 3.45 (d, 2H, CH_2, $^3J_{HH}$ = 13.3 Hz), 3.12 (d, 2H, CH_2, $^3J_{HH}$ = 13.3 Hz); ^{13}C NMR (125.7 MHz, methanol-d_4, 298 K) δ 195.1 (s, 2C, CO), 126.3 (q, 2C, CF_3, $^1J_{CF}$ = 291 Hz), 125.2 (q, 2C, CF_3, $^1J_{CF}$ = 286 Hz,), 84.2 (m, 2C, $C(CF_3)_2$, $^2J_{CF}$ = 28.0 Hz), 50.5 (s, NCH_2, 2C); ^{19}F NMR (470.3 MHz, methanol-d_4, 298 K) δ −77.36 (q, 6F, CF_3, $^4J_{FF}$ = 8.5 Hz), −77.55 (q, 6F, CF_3, $^4J_{FF}$ = 8.5 Hz). Anal. Calcd for $C_{10}H_8F_{12}N_2O_4Ru$: C, 21.87; H, 1.47; N, 5.10. Found: C, 21.54; H, 1.59; N, 4.78.

Synthesis of Complex 2. A 160 mL stainless steel autoclave was charged with 1.03 g of amino alcohol (amak2)H, $HOC(CF_3)_2CH_2NHMe$ (4.86 mmol), 0.5 g of $Ru_3(CO)_{12}$ (0.78 mmol), and 40 mL of hexane. The autoclave was sealed, and the mixture was heated to 180 °C for 18 h. The red-orange

(9) Meda, L.; Breitkopf, R. C.; Haas, T. E.; Kirss, R. U. *Mater. Res. Soc. Symp. Proc.* **1998**, *495*, 75.

(10) (a) Senzaki, Y.; Gladfelter, W. L.; McCormick, F. B. *Chem. Mater.* **1993**, *5*, 1715. (b) Senzaki, Y.; Colombo, D.; Gladfelter, W. L.; McCormick, F. B. *Proc.—Electrochem. Soc.* **1997**, *97-25*, 933.

(11) (a) Aoyama, T.; Eguchi, K. *Jpn. J. Appl. Phys.* **1999**, *38*, L1134. (b) Nabatame, T.; Hiratani, M.; Kadoshima, M.; Shimamoto, Y.; Matsui, Y.; Ohji, Y.; Asano, I.; Fujiwara, T.; Suzuki, T. *Jpn. J. Appl. Phys.* **2000**, *39*, L1188. (c) Matsui, Y.; Hiratani, M.; Nabatame, T.; Shimamoto, Y.; Kimura, S. *Electrochem. Solid-State Lett.* **2002**, *5*, C18. (d) Kim, J. J.; Jung, D. H.; Kim, M. S.; Kim, S. H.; Yoon, D. Y. *Thin Solid Films* **2002**, *409*, 28.

(12) (a) Lee, F.-J.; Chi, Y.; Hsu, P.-F.; Chou, T.-Y.; Liu, C.-S.; Peng, S.-M.; Lee, G.-H. *Chem. Vap. Deposition* **2001**, *7*, 99. (b) Chi, Y.; Lee, F.-J.; Liu, C.-S. U.S. Patent 6,303,809, 2001.

(13) Chen, R.-S.; Huang, Y.-S.; Chen, Y.-L.; Chi, Y. *Thin Solid Films* **2002**, *413*, 85.

(14) Albers, M. O.; Ashworth, T. V.; Oosthuizen, H. E.; Singleton, E. *Inorg. Synth.* **1989**, *26*, 68.

(15) Chi, Y.; Ranjan, S.; Chou, T.-Y.; Liu, C.-S.; Peng, S.-M.; Lee, G.-H. *J. Chem. Soc., Dalton Trans.* **2001**, 2462.

solution was then concentrated to dryness, and the crude product was purified by sublimation at 80 °C under a pressure of 150 mTorr, giving a light yellow solid. Recrystallization from a mixture of CH_2Cl_2 and heptane at room temperature afforded 0.51 g of colorless, needle-shaped compound $[Ru(CO)_2(amak2)_2]$ (**2**; 0.88 mmol, 38%).

Spectral data of **2**: MS (EI, ^{102}Ru) *m*/*z* 578 (M^+); IR (C_6H_{12}) ν(CO) 2042 (s), 1967 (vs) cm^{-1}; ^1H NMR (400 MHz, $CDCl_3$, 298 K) δ 4.49 (br, 2H, NH), 3.46 (dd, 2H, CH_2, $^2J_{HH}$ = 13.2 Hz , $^3J_{HH}$ = 3.6 Hz), 3.08 (dd, 2H, CH_2, $^2J_{HH}$ = 13.2 Hz , $^3J_{HH}$ = 12.4 Hz), 2.87 (d, 6H, NCH_3, $^3J_{HH}$ = 9.2 Hz); ^{13}C NMR (125.7 MHz, $CDCl_3$, 298 K) δ 193.6 (s, 2C, CO), 124.0 (q, 2C, CF_3, $^1J_{CF}$ = 290 Hz,), 123.7 (q, 2C, CF_3, $^1J_{CF}$ = 291 Hz,), 83.4 (m, 2C, $C(CF_3)_2$, $^2J_{CF}$ = 28.0 Hz), 62.5 (s, CH_2, 2C), 46.5 (s, NCH_3, 2C); ^{19}F NMR (470.3 MHz, methanol-d_4, 298 K) δ −78.13 (q, 6F, CF_3, $^4J_{FF}$ = 9.7 Hz), −78.88 (q, 6F, CF_3, $^4J_{FF}$ = 9.7 Hz). Anal. Calcd for $C_{12}H_{12}F_{12}N_2O_4Ru$: C, 24.97; H, 2.10; N, 4.85. Found: C, 24.74; H, 2.29; N, 4.73.

Synthesis of Complex 3. Sodium hydride (0.07 g, 2.9 mmol) was suspended in 25 mL of tetrahydrofuran (THF). To this was added dropwise 0.38 g of amino alcohol (amak1)H, $HOC(CF_3)_2CH_2NH_2$ (5 mmol), in THF (25 mL). The mixture was stirred for 40 min until the evolution of gas had ceased. The solution was filtered to remove the unreacted NaH. The filtrate was then transferred into a 100 mL reaction flask containing a suspension of $[Ru(COD)Cl_2]_x$ (0.15 g, 0.55 mmol) in a THF solution (25 mL). This mixture was refluxed for 48 h, giving a brown homogeneous solution along with an off-white NaCl precipitate. The precipitate was then removed by filtration, the filtrate was concentrated to dryness, and the residue was purified by column chromatography, eluting with ethyl acetate. Finally, vacuum sublimation (0.25 Torr, 150 °C) gave 0.23 g of light yellow complex [Ru(COD)(amak1)$_2$] (**3**; 38 mmol, 70%). Single crystals suitable for XRD study were grown from a mixture of ethyl acetate and pentane at room temperature.

Spectral data of **3**: MS (EI, ^{102}Ru) *m*/*z* 602 (M^+); ^1H NMR (300 MHz, acetone-d_6, 298 K) δ 5.37 (s, 2H, NH), 5.18 (s, 2H, NH), 3.63 (m, 4H, NCH_2), 3.38 (m, 2H, $CH_{(COD)}$), 3.30 (m, 2H, $CH_{(COD)}$), 2.51 (m, 2H, $CH_{2(COD)}$), 2.30 (m, 2H, $CH_{2(COD)}$), 2.15 (m, 2H, $CH_{2(COD)}$), 1.81 (m, 2H, $CH_{2(COD)}$); ^{13}C NMR (125.7 MHz, acetone-d_6, 298 K) δ 124.9 (q, 2C, CF_3, $^1J_{CF}$ = 296 Hz), 124.6 (q, 2C, CF_3, $^1J_{CF}$ = 292 Hz), 83.2 (m, 2C, $C(CF_3)_2$, $^2J_{CF}$ = 26 Hz), 79.4 (s, 2C, $CH_{(COD)}$), 76.5 (s, 2C, $CH_{(COD)}$), 52.2 (s, 2C, NCH_2), 30.3 (s, 2C, $CH_{2(COD)}$), 28.3 (s, 2C, $CH_{2(COD)}$); ^{19}F NMR (470.3 MHz, acetone-d_6, 298 K) δ −76.60 (s, 6F, CF_3), −76.62 (s, 6F, CF_3). Anal. Calcd for $C_{16}H_{20}F_{12}N_2O_2Ru$: C, 31.95; H, 3.35; N, 4.66. Found: C, 32.12; H, 3.80; N, 4.60.

Synthesis of Complex 4. The procedures were identical to those of **3** except using 0.16 g of sodium hydride (6.7 mmol), 1.03 g of the amino alcohol (amak3)H, $HOC(CF_3)_2CH_2NHEt$ (4.58 mmol), and 0.46 g of $[Ru(COD)Cl_2]_x$ (1.69 mmol). After removal of the THF solvent, the crude product was purified using column chromatography (CH_2Cl_2:hexane = 1:2), followed by sublimation (0.25 Torr, 90 °C), giving an orange solid [Ru(COD)(amak3)$_2$] (**4**; 0.85 g, 1.29 mmol) in 76% yield. Single crystals suitable for XRD studies were obtained from a mixed solution of acetone and hexane at room temperature.

Spectral data of **4**: MS (EI, ^{102}Ru) *m*/*z* 658 (M^+); ^1H NMR (400 MHz, $CDCl_3$, 298 K) δ 4.09 (m, 2H, $CH_{(COD)}$), 3.69 (m, 2H, $CH_{(COD)}$), 3.47 (m, 2H, CH_2CH_3, $^3J_{HH}$ = 7.2 Hz), 3.40 (m, 2H, NCH_2), 2.80 (s, 2H, NH), 2.66 (m, 2H, NCH_2), 2.53 (m, 2H, $CH_{2(COD)}$), 2.20 (m, 2H, $CH_{2(COD)}$), 2.08 (m, 2H, CH_2CH_3, $^3J_{HH}$ = 7.2 Hz), 2.06 (m, 2H, $CH_{2(COD)}$), 1.81 (m, 2H, $CH_{2(COD)}$), 1.17 (t, 6H, CH_3, $^3J_{HH}$ = 7.2 Hz); ^{13}C NMR (125.7 MHz, $CDCl_3$, 298 K) δ 125.4 (q, 2C, CF_3, $^1J_{CF}$ = 293 Hz), 124.1 (q, 2C, CF_3, $^1J_{CF}$ = 291 Hz), 93.9 (s, 2C, $CH_{(COD)}$), 85.4 (m, 2C, $C(CF_3)_2$, $^2J_{CF}$ = 27 Hz), 82.2 (s, 2C, $CH_{(COD)}$), 53.8 (s, 2C, NCH_2), 45.9 (s, 2C, CH_2CH_3), 30.9 (s, 2C, $CH_{2(COD)}$), 27.2 (s, 2C, $CH_{2(COD)}$), 13.9 (s, 2C, CH_3); ^{19}F NMR (470.3 MHz, $CDCl_3$, 298 K) δ −76.81 (q, 6F, CF_3, $^4J_{FF}$ = 10.8 Hz), −77.50 (q, 6F, CF_3, $^4J_{FF}$ = 10.8 Hz). Anal. Calcd for $C_{20}H_{28}F_{12}N_2O_2Ru$: C, 36.53; H, 4.29; N, 4.26. Found: C, 36.42; H, 4.30; N, 4.44.

Synthesis of Complex 5. In a fashion similar to that of **3**, 0.07 g of sodium hydride (2.92 mmol), 0.51 g of the amino alcohol (amak4)H, $HOC(CF_3)_2CH_2NH(CH_2)_2OMe$ (1.85 mmol), and 0.2 g of $[Ru(COD)Cl_2]_x$ (0.71 mmol) were used. After removal of the THF solvent, the crude product was purified using column chromatography (CH_2Cl_2:hexane = 1:2), followed by sublimation (0.45 Torr, 115 °C), giving an orange solid [Ru(COD)(amak4)$_2$] (**5**; 0.37 g, 0.51 mmol) in 72% yield.

Spectral data of **5**: MS (EI, ^{102}Ru) *m*/*z* 718 (M^+); ^1H NMR (500 MHz, $CDCl_3$, 298 K) δ 4.05 (m, 2H, $CH_{(COD)}$), 3.69 (m, 2H, $CH_{(COD)}$), 3.57 (m, 2H, CH_2CH_2), 3.52 (m, 4H, CH_2CH_2), 3.47 (m, 2H, NCH_2), 3.39 (m, 2H, NH), 3.35 (s, 6H, OCH_3), 2.73 (m, 2H, NCH_2), 2.55 (m, 2H, $CH_{2(COD)}$), 2.21 (m, 2H, CH_2CH_2), 2.20 (m, 2H, $CH_{2(COD)}$), 2.07 (m, 2H, $CH_{2(COD)}$), 1.79 (m, 2H, $CH_{2(COD)}$); ^{13}C NMR (125.7 MHz, $CDCl_3$, 298 K) δ 125.2 (q, 2C, CF_3, $^1J_{CF}$ = 292 Hz), 124.2 (q, 2C, CF_3, $^1J_{CF}$ = 291 Hz), 94.0 (s, 2C, $CH_{(COD)}$), 85.2 (m, 2C, $C(CF_3)_2$, $^2J_{CF}$ = 27 Hz), 81.8 (s, 2C, $CH_{(COD)}$), 69.9 (s, 2C, OCH_3), 59.2 (s, 2C, CH_2OCH_3), 54.4 (s, 2C, NCH_2), 50.0 (s, 2C, CH_2CH_2), 31.0 (s, 2C, $CH_{2(COD)}$), 27.2 (s, 2C, $CH_{2(COD)}$); ^{19}F NMR (470.3 MHz, $CDCl_3$, 298 K) δ −76.87 (q, 6F, CF_3, $^4J_{FF}$ = 10.4 Hz), −77.54 (q, 6F, CF_3, $^4J_{FF}$ = 10.8 Hz). Anal. Calcd for $C_{22}H_{32}F_{12}N_2O_4Ru$: C, 36.82; H, 4.50; N, 3.90. Found: C, 36.68; H, 4.66; N, 4.22.

X-ray Crystallography. Single-crystal XRD data were measured on a Nonius Kappa or a Bruker SMART CCD diffractometer using λ(Mo Kα) radiation (λ = 0.710 73 Å). The data collection was executed using the SMART program. Cell refinement and data reduction were carried out using the SAINT program. The structure was determined using the SHELXTL/PC program and refined using full-matrix least squares. All non-hydrogen atoms were refined anisotropically, whereas hydrogen atoms were placed at the calculated positions and included in the final stage of refinements with fixed parameters. Crystallographic refinement parameters of complexes **1**, **3,** and **4** are summarized in Table 1, and the selective bond distances and angles of these complexes are listed in Tables 2−4, respectively.

CVD Procedures. These reactions were carried out using a vertical cold-wall reactor described elsewhere.[16] The mixed argon gas containing 2% O_2 was purchased from a local supplier, and its compositional ratio was checked by gas chromatography. The flow rate of the carrier gas was adjusted to 10 sccm, and the sample reservoir was loaded with approximately 30 mg of the source reagent, while the typical deposition time was set to 30−40 min. Before each experiment, the Si wafers were rinsed with a diluted aqueous solution of Buffered Oxide Etch 6:1 (J. T. Baker), followed by deionized water and acetone in sequence, and dried under nitrogen.

Results and Discussion

Synthesis and Spectral Characterization. It has been reported that either neutral β-diketone or anionic β-diketonate fragments can effectively react with various metal sources to give diketonate complexes with stable metal−chelate interactions. For the β-diketonate ligand fragments containing at least one CF_3 substituent, the resulting metal complexes show a substantial increase in both thermal and chemical stability due to the electron-withdrawing effect of the fluorinated substituents which strengthen the bonding between the metal and the ligand.[17] In addition, the CF_3 substituent also possesses a notable capability of reducing the van der Waals attractive force between individual molecules,

(16) (a) Yu, H.-L.; Chi, Y.; Liu, C.-S.; Peng, S.-M.; Lee, G.-H. *Chem. Vap. Deposition* **2001**, *7*, 245. (b) Chen, Y.-L.; Liu, C.-S.; Chi, Y.; Carty, A. J.; Peng, S.-M.; Lee, G.-H. *Chem. Vap. Deposition* **2002**, *8*, 17. (c) Chi, Y.; Yu, H.-L.; Ching, W.-L.; Liu, C.-S.; Chen, Y.-L.; Chou, T.-Y.; Peng, S.-M.; Lee, G.-H. *J. Mater. Chem.* **2002**, *12*, 1363.

(17) This statement is valid for the ruthenium complexes with a metal oxidation state of +2. However, their bond strengths are also greatly affected by the nature of metal ions; for example, $Ir(acac)_3$ is highly stable, but the corresponding hfac complex $Ir(hfac)_3$ has not yet been prepared.

Table 1. Crystal Data and Structure Refinement Parameters for Complexes 1, 3, and 4

	1	**3**	**4**
empirical formula	$C_{10}H_8F_{12}N_2O_4Ru \cdot 2CH_4O$	$C_{16}H_{20}F_{12}N_2O_2Ru$	$C_{20}H_{28}F_{12}N_2O_2Ru \cdot C_3H_6O$
formula weight	613.34	601.41	715.59
diffractometer	Nonius Kappa	Bruker SMART	Nonius Kappa
temperature (K)	150(1)	295(2)	150(1)
crystal system	orthorhombic	monoclinic	orthorhombic
space group	*Pbcn*	*C*2/*c*	*Pbca*
a (Å)	17.4585(3)	17.8909(4)	8.5851(1)
b (Å)	9.9702(1)	10.0354(2)	19.8223(2)
c (Å)	12.2534(2)	11.5944(3)	32.9218(3)
β		106.8017(4)	
volume (Å^3), *Z*	2132.88(5), 4	1974.79(8), 4	5602.5(1), 8
density(calcd) (mg/m^3)	1.910	2.023	1.697
absorption coefficient (mm^{-1})	0.870	0.923	0.668
F(000)	1208	1192	2896
crystal size (mm^3)	0.30 × 0.25 × 0.25	0.30 × 0.22 × 0.20	0.30 × 0.25 × 0.20
Θ range (deg)	2.33−27.50	2.36−27.50	1.24−27.50
reflections collected	10 252	10 240	28 786
independent reflections	2446 [*R*(int) = 0.0415]	2270 [*R*(int) = 0.0177]	6409 [*R*(int) = 0.0554]
data/restraints/parameters	2446/0/154	2270/0/151	6409/0/371
goodness of fit on F^2	1.153	1.056	1.100
final *R* indices [$I > 2\sigma(I)$]	$R_1 = 0.0354$, $wR_2 = 0.0817$	$R_1 = 0.0209$, $wR_2 = 0.0552$	$R_1 = 0.0395$, $wR_2 = 0.0849$
R indices (all data)	$R_1 = 0.0655$, $wR_2 = 0.1080$	$R_1 = 0.0230$, $wR_2 = 0.0558$	$R_1 = 0.0758$, $wR_2 = 0.1085$
largest diff. peak and hole (e Å^{-3})	1.189 and −0.586	0.354 and −0.563	1.010 and −0.662

making these complexes relatively more volatile than their nonfluorinated analogues.[18] As a result, many metal complexes with fluorinated diketonate ligands have been tested and used as possible MOCVD precursors.

A second group of ligands that react like these β-diketone molecules is a class of fluoro alcohol molecules with a pendant amine functional group that is denoted as (amak)H ligands.[19] Their structures are schematically depicted in Chart 2, along with the

Chart 2

(hfac)H (amak)H: R = H, Me, Et, $(CH_2)_2OMe$

structure of the well-known acetylacetonate ligand (hfac)H. The chelation of an (amak)H ligand occurs by attachment of the amino group and the ionized alkoxy group to the cationic metal center, giving a stable five-membered metallacycle arrangement.[20] Because these fluoro alcohol ligands possess two electron-withdrawing CF_3 groups, the acidity ($pK_a = 5.35-6.39$)[16] and reactivity would be enhanced to a level comparable to that of amino acids, and thus these complexes are very suitable for the preparation of volatile metal chelate complexes that may be useful for MOCVD applications.

The synthesis of these fluorinated amino alkoxide complexes can be easily achieved via direct reaction between $Ru_3(CO)_{12}$ and an excess of the fluoro alcohol at higher temperatures, which allows the isolation of the expected mononuclear ruthenium complexes [Ru(CO)$_2$(amak1)$_2$] (**1**) and [Ru(CO)$_2$(amak2)$_2$] (**2**) in moderate yields (Chart 1). The first compound involves parent amino alkoxide (amak1) ligand fragments with R = H, while the second contains the respective *N*-methyl-substituted ligand fragments (amak2). For the synthesis of the respective COD complexes, the reaction was conducted in a THF solution, using the in situ prepared sodium salt of the fluorinated amino alcohols and the ruthenium chloride compound $[Ru(COD)Cl_2]_x$. These reactions required a longer time period (48 h) at a temperature of 66 °C, affording three complexes, namely, [Ru(COD)(amak1)$_2$] (**3**), [Ru(COD)(amak3)$_2$] (**4**), and [Ru(COD)(amak4)$_2$] (**5**), which were purified by a consecutive manipulation involving vacuum sublimation and recrystallization. Complexes **3**−**5** are isolated in yields of 70−76%, which are significantly higher than those observed in the reactions with $Ru_3(CO)_{12}$. These increased yields could be due to the lower reaction temperature, which reduced the amount of decomposition of both reactant and product. Interestingly, regardless of the conditions used, both treatment of $Ru_3(CO)_{12}$ with the distinctive fluoro alcohol $HOC(CF_3)_2CH_2NMe_2$ that possesses the tertiary amine group and reactions of $[Ru(COD)Cl_2]_x$ with the respective sodium alkoxide $Na[OC(CF_3)_2CH_2NMe_2]$ gave no evidence for the formation of any stable ruthenium complexes. It is possible that the larger steric bulkiness of the tertiary amine group altered the reaction pattern by destabilizing the N → Ru dative bonding. Moreover, the COD complex **4** also failed to react with pressurized carbon monoxide at higher temperatures (500 psig, 120 °C, 30 min), suggesting that the COD ligand may possess an even stronger ligand-to-metal dative interaction in this class of compounds.

All complexes were characterized using routine spectroscopic methods such as mass spectrometry, IR, and ^{1}H and ^{13}C NMR. For the carbonylmetal complexes **1** and **2**, the IR spectrum exhibits two strong ν(CO) stretching bands in the area of terminal CO ligands. Moreover, the CO stretching bands of **1** occurred at 2050 and 1972 cm^{-1}, which are slightly higher than those of

(18) (a) Martynova, T. N.; Nikulina, L. D.; Logvinenko, V. A. *J. Therm. Anal.* **1990**, *36*, 203. (b) Igumenov, I. K.; Belosludov, V. R.; Stabnikov, P. A. *J. Phys. IV* **1999**, *9*, 15. (c) Fahlman, B. D.; Barron, A. R. *Adv. Mater. Opt. Electron.* **2000**, *10*, 223.

(19) (a) Chang, I.-S.; Willis, C. J. *Can. J. Chem.* **1977**, *55*, 2465. (b) Willis, C. J. *Coord. Chem. Rev.* **1988**, *88*, 133.

(20) (a) Hsu, P.-F.; Chi, Y.; Lin, T.-W.; Liu, C.-S.; Carty, A. J.; Peng, S.-M. *Chem. Vap. Deposition* **2001**, *7*, 28. (b) Chi, Y.; Hsu, P.-F.; Liu, C.-S.; Ching, W.-L.; Chou, T.-Y.; Carty, A. J.; Peng, S.-M.; Lee, G.-H.; Chuang, S.-H. *J. Mater. Chem.* **2002**, *12*, 3541.

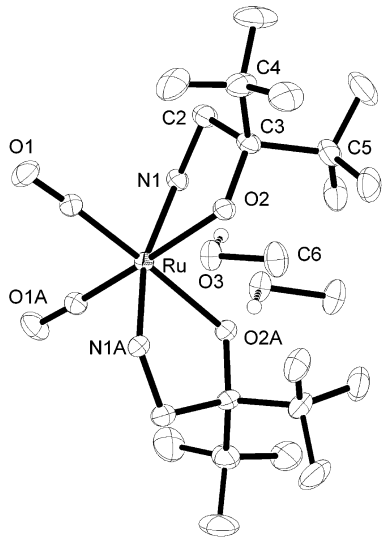

Figure 1. ORTEP diagram of complex **1** with thermal ellipsoids shown at 30% probability.

Table 2. Selected Bond Lengths (Å) and Angles (deg) for Complex 1

Ru−O(2)	2.082(2)	Ru−N(1)	2.104(2)
Ru−C(1)	1.861(3)	N(1)−C(2)	1.480(4)
O(2)−C(3)	1.379(5)	C(2)−C(3)	1.546(5)
O(1)−C(1)	1.145(4)	O(2)−O(3)	2.602(4)
∠C(1)−Ru−C(1A)	90.2(2)	∠C(1)−Ru−N(1)	94.6(1)
∠C(1)−Ru−O(2)	91.5(1)	∠C(1)−Ru−O(2A)	174.5(1)
∠N(1)−Ru−O(2)	79.19(9)	∠N(1)−Ru−N(1A)	165.8(1)

2 (i.e., 2042 and 1972 cm^{-1}), showing the greater electron-donating properties of the NHMe group. On the other hand, the ^1H, ^{13}C, and ^{19}F NMR spectra of these compounds were representative of pure, single compounds because the spectrum of each compound had shown only one set of signals for the chelating amino alkoxide ligands. In good agreement with the IR ν(CO) data obtained for the carbonyl complexes **1** and **2**, two distinct CF_3 signals were observed in the ^{19}F NMR spectra of all Ru complexes, whether or not their ligands had symmetrical NH_2 pendants. As a result, this observation gave a clear indication that the amino alkoxides were cis-oriented with respect to each other because there was no mirror symmetry passing the molecule.

Solid-State Structure. Single-crystal XRD studies were carried out to reveal their molecular structures. As indicated in Figure 1, the structure of **1** has ideal C_2 symmetry and shows an octahedral coordination about the Ru atom. The amino alkoxide ligands form five-membered chelate ring structures with the trans(N,N) amine fragments, while the cis(O,O) alkoxy fragments occupy the sites trans to the CO ligands arranged in cis(C,C) fashion. Bond length and bond angle data are given in Table 2. Metal−ligand distances found in this complex are within the range expected for octahedral Ru(II) complexes.[21] The major deviation from perfect octahedral coordination [cf. ∠N(1)−Ru−N(1A) = 165.8(1)°] is caused by the small bite angle [79.19(9)°] of the amino alkoxide chelates. The overall ligand arrangement in **1** resembles that of the structurally characterized $[Ru(CO)_2(1,2\text{-naphthoquinone-1-oximate})_2]$[22] and $[Ru(CO)_2(2\text{-pyridylcarboxylate})_2]$,[23] both of which contained a pair of cis carbonyl ligands and with the oxygen and nitrogen donor atoms located in the remainder of the coordination sites. Moreover, the alkoxy oxygen atoms in **1** are found to associate with the oxygen atom of the methanol solvate with a distance O(2)−O(3) = 2.602(4) Å, which is within the range expected for strong H bonding. It is obvious that, although the electron-withdrawing CF_3 groups have a tendency to reduce the charge density on the nearby alkoxide oxygen atom, its lone-pair electrons still can interact with the proton of methanol that was added during recrystallization, giving the observed solvate crystals.

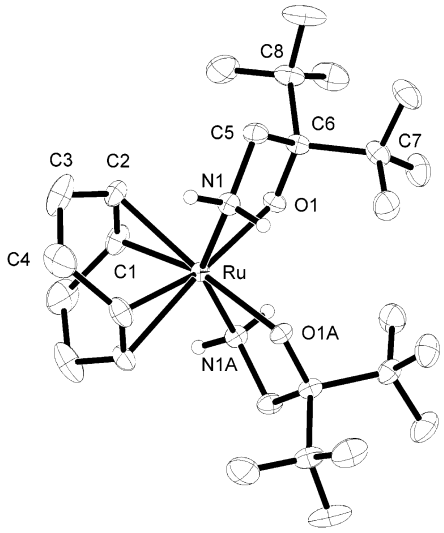

Figure 2. ORTEP drawing of complex **3** with thermal ellipsoids shown at 30% probability.

Table 3. Selected Bond Lengths (Å) and Angles (deg) for Complex 3

Ru−O(1)	2.120(1)	Ru−N(1)	2.118(1)
Ru−C(1)	2.163(2)	Ru−C(2)	2.176(2)
C(1)−C(2)	1.389(3)	C(2)−C(3)	1.495(3)
C(3)−C(4)	1.495(4)	C(1)−C(4A)	1.512(4)
O(1)−C(6)	1.371(2)	N(1)−C(5)	1.485(2)
C(5)−C(6)	1.555(2)	O(1)···N(1)	3.296(4)
∠N(1)−Ru−N(1A)	146.85(8)	∠O(1)−Ru−O(1A)	92.85(7)
∠N(1)−Ru−O(1)	77.82(5)	∠N(1)−Ru−O(1A)	79.50(5)

A perspective view of the COD complex **3** together with the atomic numbering scheme is illustrated in Figure 2. Selected bond lengths and angles are given in Table 3. The structure also has ideal C_2 symmetry, but the coordination environment about the Ru atom shows a severe distortion from the ideal octahedron. This is revealed by the detection of a small N(1)−Ru−N(1A) angle [146.85(8)°], which is significantly deviated from linearity. The amino alkoxide ligands of **3** adopt the cis(O,O) and trans(N,N) arrangement. The Ru−O(alkoxy) bond in **3** [Ru−O(1) = 2.120(1) Å] is longer than the Ru−O(alkoxy) bond in **1** [Ru−O(2) = 2.082(2)

(21) (a) Melendez, E.; Ilarraza, R.; Yap, G. P. A.; Rheingold, A. L. *J. Organomet. Chem.* **1996**, *522*, 1. (b) Baird, I. R.; Rettig, S. J.; James, B. R.; Skov, K. A. *Can. J. Chem.* **1999**, *77*, 1821. (c) Bennett, M. A.; Chung, G.; Hockless, D. C. R.; Neumann, H.; Willis, A. C. *J. Chem. Soc., Dalton Trans.* **1999**, 3451. (d) Shiu, K.-B.; Yu, S.-J.; Wang, Y.; Lee, G.-H. *J. Organomet. Chem.* **2002**, *650*, 37.

(22) Lee, K. K.-H.; Wong, W.-T. *J. Chem. Soc., Dalton Trans.* **1997**, 2987.

(23) Xu, L.; Sasaki, Y. *J. Organomet. Chem.* **1999**, *585*, 246.

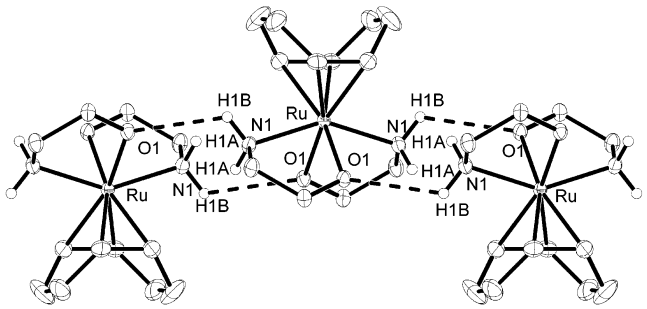

Figure 3. 2D packing arrangement of complex **3**, on which the CF_3 substituents were removed for clarity.

Å], while the variation of the Ru−N distances with respect to those of complexes **1** and **3** is relatively less significant [0.014(2) Å]. This may be due to the fact that the olefinic C−C double bond of the COD ligand possesses a slightly larger trans influence compared with that of terminal CO ligands in this class of compounds. Thus, the donor atoms residing opposite to the COD olefin fragments experience a much more notable effect of bond lengthening. Moreover, Figure 3 shows a two-dimensional packing arrangement of **3** within the solid state. It is obvious that each individual molecule has now interacted with its neighboring molecules through a total of four N−H···O bonding interactions with distance O(1)···N(1) = 3.296(4) Å. Although these nonbonding contacts are longer than those found for the medium-strong N−H···O bonds observed in typical coordination complexes (O···N = 2.69−2.79 Å)[24] as well as the cyclic copper decamer $[CuClL]_{10}$ with L = OC-$(CF_3)_2CH_2NHCH_2CH_2NMe_2$ (O···N = 2.834(1)−2.905-(2) Å),[25] the quantity (i.e., the total number of H-bonding interactions per molecule) has obviously compensated the weak stabilization provided by each of the individual N−H···O bondings.

Moreover, the crystal structure of **4**, for which its ligand contains secondary amine fragment NHEt, was determined in an attempt to reveal the possible influence of the amino group. Its ORTEP plot is depicted in Figure 4, showing the expected coordination arrangement involving one COD ligand and two amino alkoxide chelates, as well as an acetone solvate residing close to the NHEt groups with distances O(3)···N(1) = 4.283(5) Å and O(3)···N(2) = 3.163(5) Å.

The selected bond distances and angles are summarized in Table 4. In contrast to the previously determined structure of complex **3**, which showed a trans(N,N) ligand arrangement, the amine groups of **4** turned to a different cis arrangement and resided at the positions trans to the C−C double bonds of the COD ligand. The O(1)−Ru−O(2) angle in **4** is 158.00(8)°, which is greater than that of the trans N(1)−Ru−N(1A) vector observed in the NH_2-substituted Ru complex **3** [146.85(8)°]. Concomitant with a change in the ligand arrangement, the Ru−N distances were elongated [i.e., Ru−N(1) = 2.201(2) Å and Ru−N(2) = 2.215(2) Å] with respect to the Ru−N distances observed in complexes **1** and **3** [2.104(2) Å and 2.118(2) Å]. Again, this bond

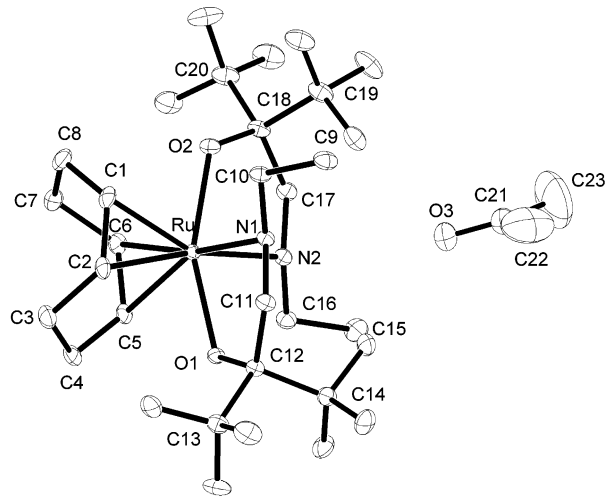

Figure 4. ORTEP drawing of complex **4** with thermal ellipsoids shown at 50% probability.

Table 4. Selected Bond Lengths (Å) and Angles (deg) for Complex 4

Ru−O(1)	2.089(2)	Ru−O(2)	2.082(2)
Ru−N(1)	2.201(2)	Ru−N(2)	2.215(2)
Ru−C(1)	2.172(3)	Ru−C(2)	2.193(3)
Ru−C(5)	2.180(3)	Ru−C(6)	2.192(3)
C(1)−C(2)	1.388(4)	C(2)−C(3)	1.520(4)
C(3)−C(4)	1.532(4)	C(4)−C(5)	1.504(4)
C(5)−C(6)	1.390(4)	C(6)−C(7)	1.521(4)
C(7)−C(8)	1.536(5)	C(1)−C(8)	1.509(4)
O(1)−C(12)	1.373(3)	N(1)−C(11)	1.479(4)
O(2)−C(18)	1.365(4)	N(2)−C(17)	1.483(4)
C(11)−C(12)	1.543(4)	C(17)−C(18)	1.545(4)
∠O(1)−Ru−O(2)	158.00(8)	∠N(1)−Ru−N(2)	89.18(9)
∠O(1)−Ru−N(1)	77.97(8)	∠O(1)−Ru−N(2)	86.63(8)
∠O(2)−Ru−N(1)	86.01(8)	∠O(2)−Ru−N(2)	78.09(8)

lengthening can be attributed to the larger trans influence imposed by the C−C double bond, with respect to the amine donor ligand of **3**. Finally, the trans(O,O) arrangement of the alkoxy oxygen atoms is analogous to that observed in complex $[Ru(COD)(quin)_2]$,[26] which was prepared in a similar manner by heating a methanol solution of $[Ru(COD)Cl_2]_x$ and anionic quinolin-8-olate.

Thermal Analysis. The volatility and thermal stability of complexes **1**−**4** were investigated by thermogravimetric analysis (TGA) under an atmospheric pressure of N_2 (Figure 5). Generally speaking, the *N*-alkyl complexes **2** and **4** are more volatile than the NH_2-substituted complexes **1** and **3**, respectively. This is revealed by a rapid loss of weight, which started at 150 °C for the *N*-methylcarbonyl complex **2** and at 190 °C for the *N*-ethyl-COD complex **4**, while the onset temperatures for the NH_2-substituted complexes **1** and **3** begin at much higher temperatures of 250−270 °C. This notable difference in volatility is probably due to the presence of N−H···O hydrogen bonding, which considerably increases the intermolecular attraction, thus lowering the volatility. Confirmation of this postulation was provided by the occurrence of H bonding between the alkoxy oxygen atom and the methanol solvate in complex **1** [O(2)···O(3) = 2.602(4) Å] and the detection of a short O···N contact between the alkoxy oxygen atom and

(24) Couchman, S. M.; Jeffery, J. C.; Ward, M. D. *Polyhedron* **1999**, *18*, 2633.

(25) Chang, C.-H.; Hwang, K. C.; Liu, C.-S.; Chi, Y.; Carty, A. J.; Scoles, L.; Peng, S.-M.; Lee, G.-H.; Reedijk, J. *Angew. Chem., Int. Ed.* **2001**, *40*, 4651.

(26) Gemel, C.; John, R.; Slugovc, C.; Mereiter, K.; Schmid, R.; Kirchner, K. *J. Chem. Soc., Dalton Trans.* **2000**, 2607.

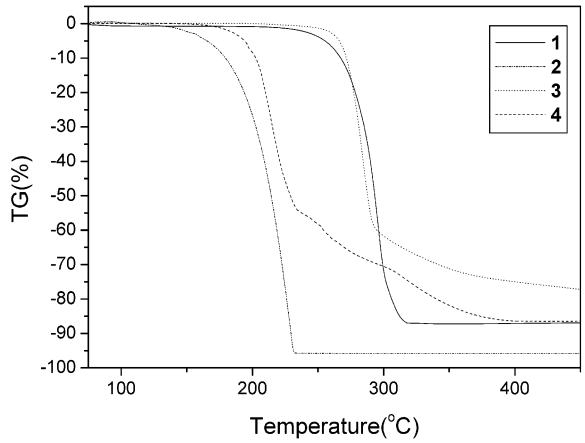

Figure 5. TGA data of complexes **1**−**4**. All experiments were carried out at atmospheric pressure with N_2 as the carrier gas (100 sccm) and with a heating rate of 10 °C/min.

Table 5. Selected Physical Properties of Complexes 1 ~ 5

compd no.	MW	mp (°C)	$T_{1/2}$ (°C)[a]	% residue[b]
1	549.93	295 (dec)	291	13.3
2	577.96	137−140	210	4.7
3	602.04	288−290	284	19.6
4	658.10	196−198	223	13.7
5	718.12	205−207	231	17.4

[a] The temperature at which 50 wt % of the sample has been lost during TGA analysis. (heating rate = 10 °C/min and N_2 flow rate = 100 cm^3/min). [b] Total weight percent of the sample observed at 500 °C during TGA analysis.

the amino fragment of nearby molecules in complex **3** [3.296(4) Å]. Moreover, although there is no direct H bonding between each of the individual molecules of **1**, its formation would become inevitable once all methanol solvates were removed by simply raising the temperature.

Other physical properties relevant to TGA experiments, such as melting points, deposition temperature, and $T_{1/2}$, which shows the temperature at which 50 wt % of sample has been lost during TGA runs, are all listed in Table 5. This systematic trend allowed us to adjust the physical properties by simply changing the ancillary ligands (i.e., carbonyl vs COD) and by varying the alkyl substituent on the amino fragments. Of particular interest is the two-stage loss of weight that was observed in complex **4** (Figure 5): the first occurred at lower temperatures, 190−230 °C, and the second started as the temperature exceeded 230 °C. The occurrence of such a two-stage process could be due to a concurrent, thermally induced ligand dissociation, for which the unsaturated reaction intermediate would undergo self-aggregation, leading to the formation of higher molecular weight, less volatile material. No attempt was made to characterize this solid residue.

CVD Experiments. The CVD experiment was then conducted on a vertical, cold-wall reactor using complex **2** as the ruthenium source reagent and high-purity H_2 as the carrier gas. We selected complex **2** as the source reagent simply because of its higher volatility and lower melting point. At 375 °C, the as-deposited thin films showed a lustrous, silver-gray color, which adhered very well to the substrate surface. A summary of deposition parameters, together with analytical data, is given in Table 6. An SEM picture is depicted in Figure 6, showing the formation of essentially featureless surface morphology. In good agreement with the amorphous nature, the XRD spectrum showed no obvious diffraction signal in the region expected for the ruthenium metal (Figure 7).

Upon a change of the carrier gas from H_2 to a mixture of 2% oxygen in argon, the formation of Ru metal was confirmed using the XRD reference signals of hexagonal Ru metal standards, although the observed signal intensities were broader than expected. In the meantime, the SEM analysis showed the formation of closely packed, granular crystallites. XPS showed a low carbon content at a level of ~1% and a slightly higher content for oxygen at ~4%, while four-point probe measurements gave a resistivity $\rho = 13.5$ $\mu\Omega$·cm, which is slightly higher than that of the bulk Ru standard (7.1 $\mu\Omega$·cm at 0 °C).[27] The success of this experiment confirmed that the deposition of metallic ruthenium is possible even under conditions using a small amount of an oxidant such as oxygen. Furthermore, the XRD pattern showed an enhanced (002) signal intensity, which is consistent with the characteristics of *C*-axis-oriented Ru thin films that were deposited on glass substrates using dc magnetron sputtering in a mixture of argon and ambient O_2.[28] This is attributed to the fact that the (001) crystallographic planes have the closest interplanar spacing and that the adsorbed oxygen atom may decrease the surface free energy and enhance the (001) preferential orientation.

The CVD experiment was also extended to a second system where complex **4** was used as the source reagent. The major reason for this examination is to probe the suitability of COD complexes as alternative source reagents for metal deposition. As can be seen from the data listed in Table 5, the as-deposited Ru thin film showed a comparable amount of impurity and a resistivity (25.3 $\mu\Omega$·cm) slightly inferior to that of the thin film obtained using carbonyl complex **2**. At 325 °C, deposition carried out under the mixed carrier gas gave an amorphous Ru thin film with certain imperfections due to the formation of a few hillocks (Figure 6). However, upon an increase in the temperature to 375 °C, the thin film obtained showed a different morphology; the SEM picture revealed an increased surface

Table 6. Summary of the CVD Experimental Data Obtained Using the Source Reagents 2 and 4[a]

entry no.	source	CGFR (sccm)	T_S (°C)	T_D (°C)	P_S (Torr)	thickness (Å)	dep rate (Å/min)	resistivity ρ ($\mu\Omega$·cm)	cont. (at. %)
1	**2**	H_2 (10)	90	375	0.25	980	25	120	C, 9%; O, 4%
2	**2**	O_2(2%)/Ar (10)	90	375	0.25	1460	42	13	C, 1%; O, 4%
3	**4**	O_2(2%)/Ar (10)	110	325	0.25	900	15	28	C, 2%; O, 1%
4	**4**	O_2(2%)/Ar (10)	110	375	0.25	1270	21	25	O, 4%
5	**4**	O_2(2%)/Ar (10)	110	425	0.25	1560	26	22	C, 1%; O, 3%

[a] CGFR: carrier gas flow rate using a mixture of 2% oxygen in argon. T_S: source temperature. T_D: deposition temperature. P_S: initial system pressure. dep rate: deposition rate. cont.: contents of nonmetal elements determined by XPS.

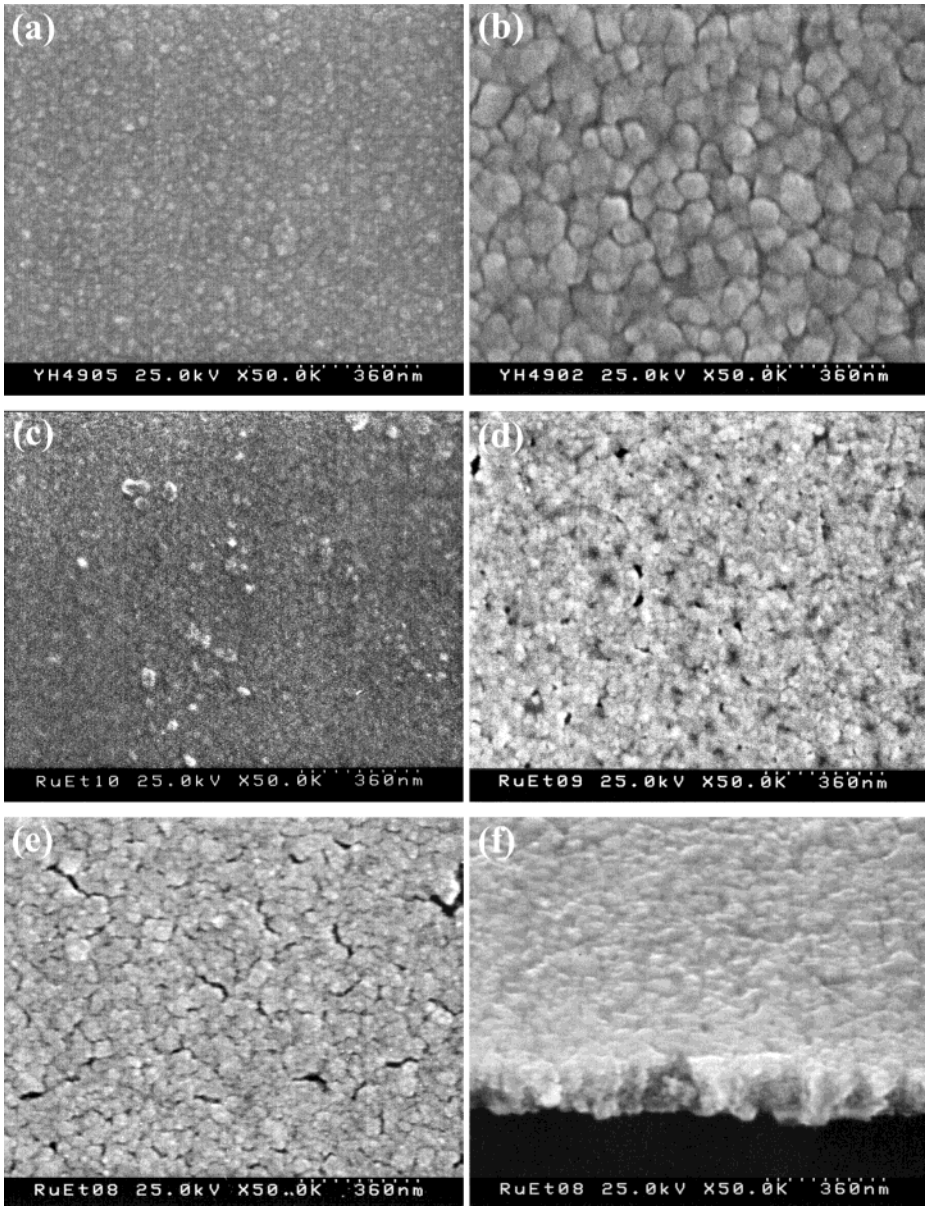

Figure 6. SEM micrographs of the as-deposited Ru metal thin films: (a) entry 1, (b) entry 2, (c) entry 3, (d) entry 4, (e) entry 5, and (f) tilt view of entry 5. The entry numbers are identical to those listed in Table 6.

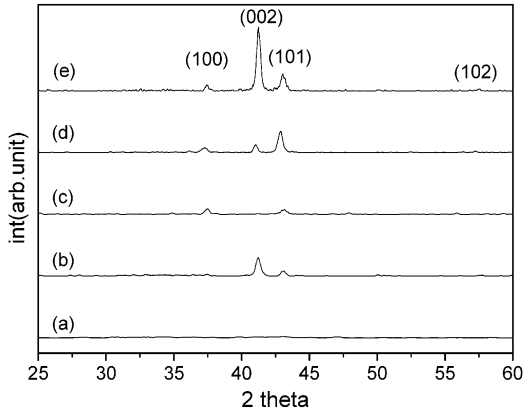

Figure 7. XRD pattern of the as-deposited Ru metal thin films. Numberings are also identical to those listed in Table 6.

roughness and the formation of voids between regions of fused crystallites. By a further increase in the temperature to 425 °C, the thin film changed to the *C*-axis orientation and the residual impurity content and resistivity were maintained at about the same levels as those observed at 375 °C, but the relative roughness had increased substantially along with an increase of its thickness. As revealed by the SEM analysis, the development of trenches and cracks between crystallites was clearly observed on the top surface, but the tilt view showed very little of such a defect. The cause of this deteriorated surface morphology is not clear, but it is probably related to the combustion of the surface-bound COD ligand during metal deposition.

Conclusion. Octahedral Ru complexes containing two amino alkoxide ligands were prepared. These metal complexes showed enhanced thermal and chemical stability, and all of these molecules can be volatilized

(27) (a) Lide, D. R. *CRC Handbook of Chemistry and Physics*; CRC Press: Boca Raton, FL, 1997; pp 12−45. (b) Green, M. L.; Gross, M. E.; Papa, L. E.; Schnoes, K. J.; Brasen, D. *J. Electrochem. Soc.* **1985**, *132*, 2677.

(28) Abe, Y.; Kaga, Y.; Kawamura, M.; Sasaki, K. *Jpn. J. Appl. Phys.* **2001**, *40*, 6956.

during TG analysis under N_2 at 1 atm and at temperatures below 250 °C. From the structural prospective, the carbonyl derivative complexes showed only one type of structure with cis carbonyl ligands and with oxygen atoms of the chelating amino alkoxides located trans to the carbonyl ligands. In contrast, the COD complexes exhibited two distorted skeletal arrangements: one with cis amine functional groups, while the second showed trans amino groups and with alkoxide oxygen atoms located cis to the COD ligand. This change of crystal structure appeared to be the result of the amine ligands, which allowed the formation of linear, intermolecular H bonding within each molecule of **3**, as shown in Figure 3.

Deposition of the Ru thin film was achieved using a H_2 carrier gas or a mixture of 2% oxygen in argon. For complex **2**, deposition of both amorphous thin films that consists of granular crystallites was obtained at 375 °C. By comparison of the impurity content of these thin films, it seems that both the fluorine and nitrogen residues were below the detection limit under all conditions and that the H_2 carrier gas was less effective in terms of the removal of carbon, compared with the mixed carrier gas involving 2% O_2, but the oxygen contamination detected during H_2 deposition appeared to be somewhat identical. Moreover, according to the literature reports,[29] CVD experiments conducted using high O_2 concentrations, i.e., under the condition employing a pure O_2 carrier gas, lead to the formation of the rutile RuO_2 phase through in situ metal oxidation, which becomes the dominant reaction pathway. It appeared that our source reagents gave the same kind of behavior; thus, the subsequent depositions were not continued.

Finally, by switching to the COD complex **4** as the alternative source reagent, Ru thin film with dense and smooth surface morphology can be obtained at temperatures as low as 325 °C. Although optimization of the deposition conditions will be necessary in the future, the basic physical properties such as resistivity are sufficiently good for applications such as capacitor electrodes.[30] Therefore, both of these complexes are promising for utilization as the next generation of Ru CVD source reagents.

Acknowledgment. Y.C. thanks the National Science Council and the Ministry of Education for financial support (NSC 91-2113-M-007-006) and (MOE program 89-FA04-AA).

Supporting Information Available: X-ray crystallographic file (CIF) for complexes **1**, **3**, and **4**. This material is available free of charge via the Internet at http://pubs.acs.org.

CM030029C

(29) (a) Smith, K. C.; Sun, Y.-M.; Mettlach, N. R.; Hance, R. L.; White, J. M. *Thin Solid Films* **2000**, *376*, 73. (b) Liao, P. C.; Huang, Y. S.; Tiong, K. K. *J. Alloys Compd.* **2001**, *317−318*, 98. (c) Frohlich, K.; Machajdik, D.; Cambel, V.; Kostic, I.; Pignard, S. *J. Cryst. Growth* **2002**, *235*, 377.

(30) (a) Choi, E.-S.; Shin, W.-C.; Suh, T.-S.; Park, S.-S.; Yoon, S.-G. *Integr. Ferroelectr.* **2000**, *31*, 297. (b) Park, K. W.; Han, Y. K.; Oh, K.; Yang, D. Y.; Hwang, C. J.; Park, J.; Hwang, C. S. *Integr. Ferroelectr.* **2000**, *30*, 45.